

A greenery-based solution for low-noise delivery hub for unmanned aerial transport

Giorgio Palma*, Claudio Pasquali, Caterina Poggi, Lorenzo Burghignoli, Jacopo Serafini

Department of Engineering, Roma Tre University, Via Vito Volterra, 62, Roma, 00146, Italy.

*giorgio.palma@uniroma3.it

Summary

Unmanned Aerial vehicles are nowadays involved in a wide range of applications, such as surveillance, safety control, scientific research, and commercial activities. The logistics industry, in particular, is showing a substantial interest in a partial transition of the last-mile delivery service from ground to air transport. A key point to make this scenario feasible resides in the design of delivery hubs to serve the surrounding areas, thus overcoming the logistical difficulties of a door-to-door delivery while respecting the strict regulations in terms of noise. The proposed paper deals with the study and design of an urban hub for package delivery that uses natural elements such as hedges to limit the noise footprint associated with drone operations by exploiting the shielding capabilities of natural barriers. Some constraints driving the design are identified, leading to a tentative conceptual design. The acoustic property of a sample hedge is evaluated using an equivalent porous medium approach, informed by parameters estimated by image processing of the external surface of the hedge. Eventually, the model is used in coupled BEM-FEM simulations of simplified designs. Preliminary results show encouraging noise reductions in the areas surrounding the hub.

1. Introduction

In the last few years, the constant growth of urban pollution and overcrowding has led to an increasing interest in alternative and sustainable solutions to conventional urban mobility. In this framework, the Urban Air Mobility (UAM) represents a possible solution made viable by the emerging technological innovations in several fields,

such as automation or electrification. Nevertheless, many open questions regarding the implementation of UAM transportation networks, such as certification, traffic management, or ground infrastructure requirements, remain answered [1]. Besides, the environmental sustainability of these Urban Aerial Vehicles (UAVs) is a fundamental condition of their entry-into-service, as well testified by the increasingly strict regulations for the whole aviation world in terms of chemical pollution and noise [2]. Many industries are nowadays involved in the design and manufacturing of innovative electric vertical takeoff and landing concepts (eVTOLs) [3]. Furthermore, several tasks, such as surveillance, safety control, and scientific research, have been in the last few years rethought in order to be accomplished by drones [4]. Moreover, UAVs are rapidly being involved in commercial activities. The logistics industry, in particular, is showing a substantial interest in a partial transition of the last-mile delivery service from ground to air transport, and different solutions have been presented by the leading actors who are showing interest in this area [5]. Delivery drones in the sky might become as common as mail trucks on the road in the near future. Nevertheless, to make this suggestive scenario feasible, a new set of infrastructures are necessary for the operations connected to drone flight tasks [6]. A typical mission of a UAV for delivery starts with the pick up of the pack, an autonomous flight ending with a hovering phase over the delivery point, and a vertical descent to drop the pack safely (max altitude 0.15-0.30 m) [7]. It is hard to imagine a drone landing spot for each consumer in the urban context. Thus, a feasible solution could be the realization of delivery hubs serving all surrounding areas. Nevertheless, the noise annoyance produced by intensive operations in localized areas, although of small drones, is a critical issue for developing urban air delivery services. In this scenario, this work deals with the study and design of an urban hub for package delivery that uses natural elements (grass, hedges, trees) to limit the noise footprint associated with drone operations. There is a growing interest in the noise shielding capabilities of natural barriers. Some works can be found in the literature on the acoustic modeling of organic barriers, mainly focused on low growing plants [8, 9, 10, 11]. A common approach considers the greenery as a porous material, presenting a rigid frame (leaves and woody parts) filled with air, which can be, in turn, characterized using different models. In [10] and [11], experiments allowed to perform optimization for the inverse characterization of the equivalent porous medium using the three-parameters Delany-Bazley-Miki model [12]. Specifically, based on the physical and geometrical properties of the plant, some semi-empirical models were derived for equivalent porosity, flow resistivity, and tortuosity. It is there highlighted how trying to measure such parameters for plants and trees directly is not a trivial task, and inverse estimation was explored as a strategy to develop reliable equivalent-medium-based modeling for plants and plant-soil combinations. Some experiments have also been performed on sound attenuation by hedges [13], measuring the insertion loss obtained at a distance of 1m from the hedge for a controlled noise source and numerically reproducing it through an equivalent porous material. It is found that a considerable noise reduction at the receiver can be obtained for hedges of 1.5m of thickness, with an effect comparable to standard acoustic barriers. To this aim, first, the acoustic properties of standard plants are evaluated, and then preliminary simulations to assess the acoustic properties of the hedge shields are performed. In particular, in Sec. 2 the guidelines followed for the delivery hub design are presented; then, in

Sec. 3 the strategy followed for the characterization of the acoustic properties of the selected barriers are explained, and the numerical results of the proposed approach for a selected configuration are shown in Sec. 4; finally, some concluding remarks are reported in Sec. 5.

2. Design of the Green delivery hub

Operational and environmental constraints influence the design of a delivery hub. A non-exhaustive list of such constraints are:

- internal space sufficient to host a landing spot and an automatic locker;
- enough space for user access and to perform maintenance;
- overall footprint below $10 \times 10 \text{ m}^2$ in order to be fitted into parks or unused urban space;
- high capacity;
- possibility to perform non-vertical takeoff to reduce required power;
- good resilience to gusts.

These constraints lead to the definition of a tentative design of the delivery hub, consisting of a number of circular hedges surrounding a landing/take-off platform. The sketch of the proposed hub in multi-hedge configuration is shown in the Fig. 1, including hedges (in green) and the operational platform (in black). Access to the hub is guaranteed by the openings present in the various layers of the hedge (visible in Fig. 1b), which are suitably misaligned to minimize the inevitable loss of acoustic performance. In addition, the hedges are designed with different heights (Fig. 1a) to form an inverted cone-shaped entrance towards the platform. This inverted cone shape is

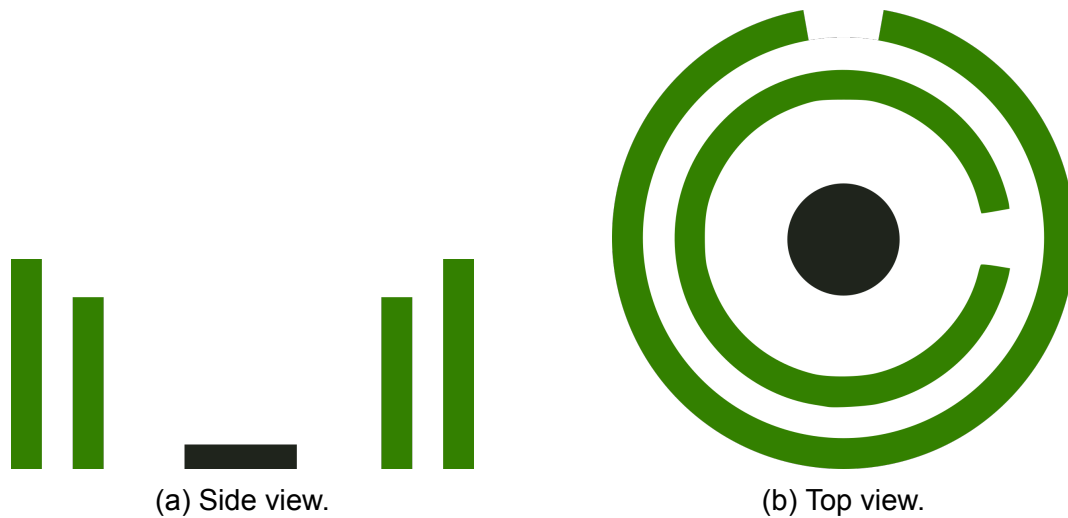


Figure 1: Sketch of the proposed delivery hub including two layers of hedges (green) and the platform for landing/take-off (black).

Name	Planform dimensions (mm)	MTOW (kg)	Payload
Wingcopter 198[14]	1520 x 1980	25	5
Swoop aero Kite[15, 16]	2400 x n.a.	n.a.	5
Alphabet Wing[17]	1300 x 1000	6.4	1.2
Amazon prime air[5]	914 x 914	7.8	2.3
Dij Matrice 600 Pro[18]	1668 x 1518	15.5	5.5

Table 1: Delivery drone dimensions.

intended to give good noise shielding performance up to a specific azimuth, allowing, at the same time, an easy and efficient landing with sufficient translational velocity. Indeed, a purely vertical take-off and landing would require more power (due to the absence of translational lift) and drastically reduce hub capacity (hourly throughput) since the maneuver is slow and the descent and climb path coincide. Furthermore, the multi-hedge configuration reduces the loss of shielding effect in the path users follow (avoiding the line of sight between the noise source and observers outside the hub) and optimizes plants' use since the leaf distribution is concentrated in the outer part of the plants. An analysis of dimensions of existing delivery drones, reported in Tab.1, helped in defining the required take-off&landing area extension. It is found that an average delivery drone has a planform that can be contained in a square box of 2.5 m side, hence it is decided that a circular area of radius 2.5m inside the inner hedge circle is needed, in order to ensure sufficient tolerances for the autonomous maneuvers.

Maintenance represents a critical aspect that, especially in a hub based on natural elements such as hedges, must be considered right from the conceptual design stages. In particular, (i) the distance between the various layers of plants must be sufficient not only for the transiting of people and their goods but also to allow the necessary thinning operations; (ii) it is necessary to ensure the presence of an adequate water network for the necessary irrigation. The main requirements that hedges must meet are: (i) they do not drop leaves during the adverse season; (ii) possibility of growing to heights equal or greater than two meters; (iii) high growth rate; (iv) resistance to local climate (extreme) conditions. The first requirement implies that the choice necessarily falls on evergreen plants, commonly used for making hedges. Among these, it is possible to identify some that meet all or part of the above requirements, for example, looking at applications in the Mediterranean and Center Europe, the *Cherry Laurel*, the *Laurel*, the *Cypress*, the *Ligustrum*, the *Pyracantha* and the *Japanese Privet*. For availability reasons, in the present study, the studied hedges is assumed to be made of *Buxus*, even though this species is not one of the most suitable.

3. Porous material model for hedges

A modified version of the well known six-parameters Johnson-Champoux-Allard model for porous media has been introduced recently[19], hereby called the JCAH model, reducing the number of independent parameters of the porous domain down to three under the assumption of log-normal distribution of pores' size, namely the porosity

Φ , the standard deviation of the pores' size σ_S , and the size of the median pores \bar{s} . Under the mentioned hypothesis, tortuosity a_∞ , flow resistivity σ and thermal flow resistivity σ' are obtained as

$$a_\infty = e^{4(\sigma_S \log 2)^2} \quad (1)$$

$$\sigma = \frac{8\eta a_\infty}{\bar{s}^2 \Phi} e^{6(\sigma_S \log 2)^2} \quad (2)$$

$$\sigma' = \frac{8\eta a_\infty}{\bar{s}^2 \Phi} e^{-6(\sigma_S \log 2)^2} \quad (3)$$

with η being the dynamic viscosity. Expressions for equivalent mass density and bulk modulus can be obtained from these parameters as:

$$\rho(\omega) = \rho_0 \frac{a_\infty}{\Phi} (1 + \epsilon_\rho^{-2} F_\rho(\epsilon_\rho)) \quad (4)$$

$$B(\omega) = \frac{\Phi}{\gamma p_0} \left(\gamma - \frac{\gamma - 1}{1 + \epsilon_B^{-2} F_B(\epsilon_B)} \right) \quad (5)$$

with

$$\epsilon_\rho = \sqrt{\frac{-i\omega \rho_0 a_\infty}{\Phi \sigma}}, \quad F_\rho(\epsilon_\rho) = \frac{1 + \theta_{\rho,3} \epsilon_\rho + \theta_{\rho,1} \epsilon_\rho^2}{1 + \theta_{\rho,3} \epsilon_\rho} \quad (6)$$

$$\theta_{\rho,1} = \frac{1}{3}, \quad \theta_{\rho,2} = \frac{e^{-\frac{1}{2}(\sigma_S \log 2)^2}}{\sqrt{2}}, \quad \theta_{\rho,3} = \frac{\theta_{\rho,1}}{\theta_{\rho,2}} \quad (7)$$

$$\epsilon_B = \sqrt{\frac{-i\omega \rho_0 \text{Pr} a_\infty}{\Phi \sigma'}}, \quad F_B(\epsilon_B) = \frac{1 + \theta_{B,3} \epsilon_B + \theta_{B,1} \epsilon_B^2}{1 + \theta_{B,3} \epsilon_B} \quad (8)$$

$$\theta_{B,1} = \frac{1}{3}, \quad \theta_{B,2} = e^{\frac{3}{2}(\sigma_S \log 2)^2}, \quad \theta_{B,3} = \frac{\theta_{B,1}}{\theta_{B,2}} \quad (9)$$

where $\gamma = c_p/c_v$, Pr is the Prandtl number and p_0 is the ambient pressure.

In this article, it is proposed that the information required for the definition of the equivalent porous material in terms of \bar{s} and σ_S can be obtained by analyzing simple pictures of the hedge, and consequent values obtained for σ are comparable to what is predicted using the method in [10], and [11].

3.1. Estimation of hedge parameters

As stated above, in this work, an algorithm to estimate \bar{s} and σ_S has been developed, which is based on an image processing of the external surface of the hedge. The main idea behind the algorithm comes from direct observation of the hedge. Due to its composition, it is a common experience that, looking at its external surface, one will see a random distribution of clear and dark areas, coming from an overlap of leaves layer which fights together to reach the light. This structure somehow represents a porous surface with a random distribution of holes. The algorithm could be outlined in the following procedure:

- i - Calibration - During the first step the pixel-to-meter scaling is obtained from the ruler inserted in the picture,

- ii - Binarization - Defining a threshold value, the original RGB or grey scale image is converted to a black and white one.
- iii - Image analysis - In the B&W converted image, the white parts represent the holes on the hedge surface. These are extracted by the processing algorithm, identifying ellipses with equivalent radius bigger than a minimum reference value.
- iv - Statistics evaluation - The data from the previous step in terms of holes equivalent radius are statistically analyzed and a fitted by a log-normal distribution. Its median \bar{s} and standard deviation σ_s are then obtained and used for the characterization of the equivalent porous material.

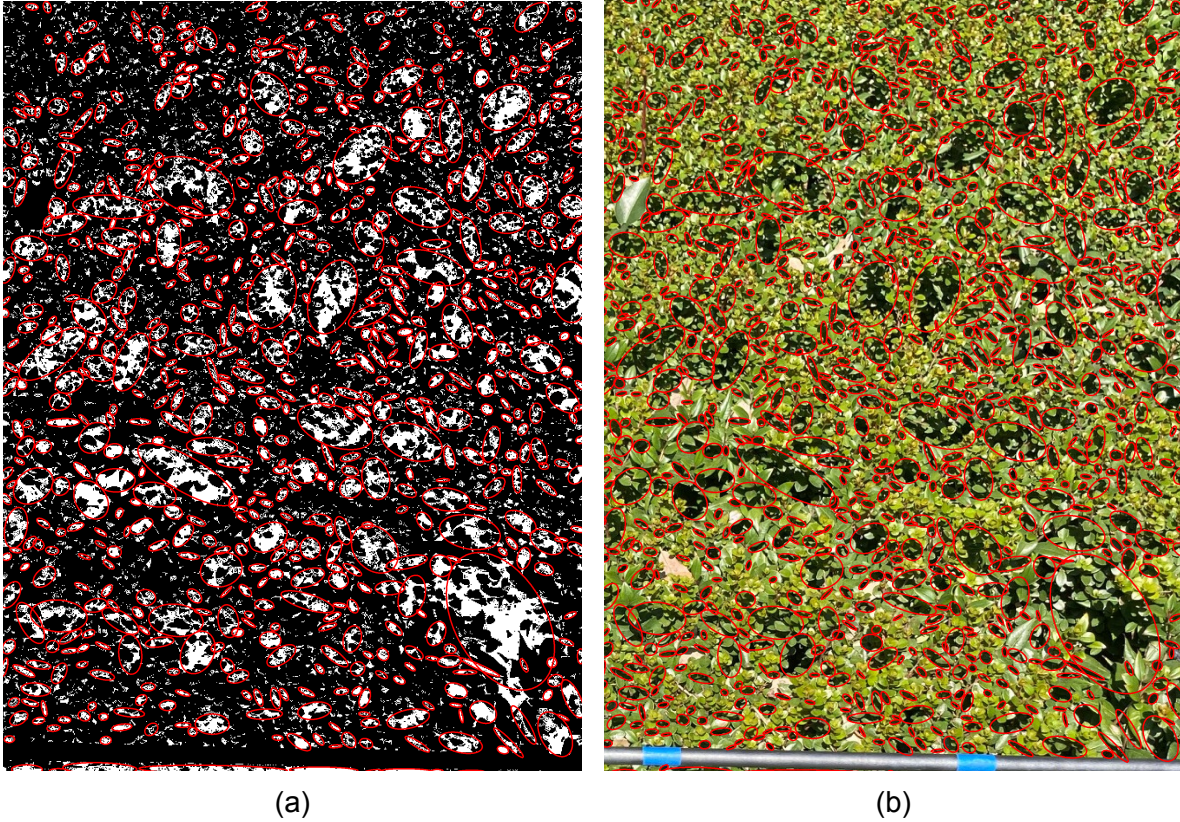


Figure 2: Binarized image with the identified holes (a). The red ellipses representing the holes are plotted over the original RGB picture (b) to verify the results of the analysis.

In Fig. 2 an application of the proposed algorithm is presented: the red ellipses in Fig. 2a represent the holes identified on the b&w image, superimposed on the original picture in Fig. 2. In particular, Fig. 2a clearly shows how the algorithm can correctly identify the equivalent holes of the hedge surface. For the sake of simplicity, the mean of the two ellipse's axes has been chosen as the radius of an equivalent circumference representing each hole. Once the ellipses are identified and their equivalent radii collected, it is possible to analyze and verify the log-normality of their distribution, Fig. 3. The evaluation of the porosity Φ has been performed starting from

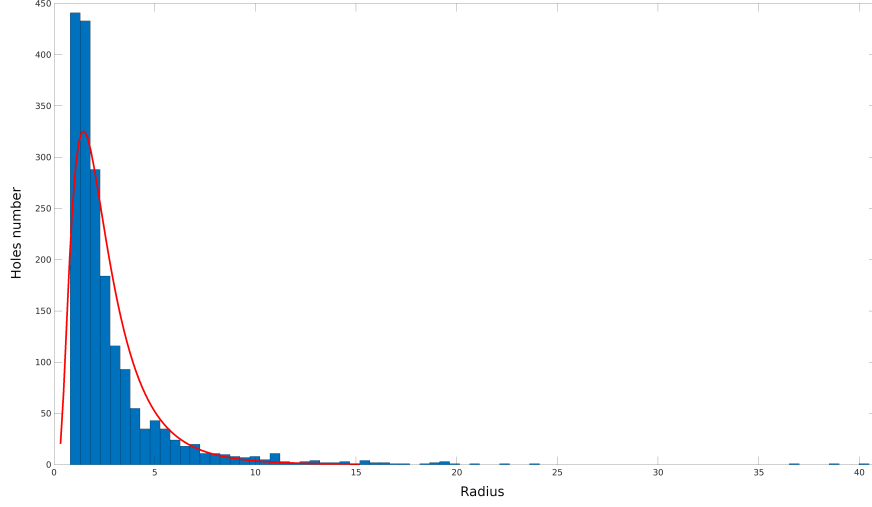


Figure 3: Probability distribution of holes equivalent radii for the Buxus hedge.

some morphological parameters of the plant: the average thickness of a representative leaf t_f , the average distance between two leaves along a branch d_f and the surface porosity $\Phi_S = \sum_{j=1}^{n_h} S_j / S_p$, defined as the ratio between the holes surface S measured from the picture and the picture surface S_p ,

$$\Phi = \frac{d_f + \Phi_S h_f}{d_f + h_f} \quad (10)$$

The obtained values have been verified with a more classic approach, following the experience reported in [10]. Other morphological parameters of the plants were measured from taken specimens of known sizes: the area of a representative leaf a_f that has been measured with the image processing technique and the number of leaves in the sample n_f that has been directly counted. In this case, starting from the volume of the sample V_p and the volume occupied by the foliage V_f , the porosity is evaluated as

$$\Phi_H = 1 - \frac{V_f}{V_p} = 1 - \frac{n_f a_f t_f}{V_p} \quad (11)$$

Values of Φ , \bar{s} and σ_S are reported in Tab. 2 for a Buxus hedge. The two approaches

Species	Φ	Φ_H	\bar{s} (m)	σ_S
Buxus	0.96	0.97	0.00246	0.655

Table 2: Plants parameters

for the evaluation of the porosity provided almost identical results for the considered specimens.

4. Numerical Results

Some preliminary simulations have been performed on simplified geometries, representative of the proposed design for the green delivery hub using the data from the Buxus hedge. In particular, to acoustically shield the landing area with a radius of 2.5m, we compared a single-layer and a two-layers design of 2m high circular hedge(s). The former has a thickness of 1.5m, placed around a landing area with a radius of 2.5m. The latter is composed of two concentric hedges with a thickness of 0.75m each; a labyrinthine path guarantees access to the landing area inside the inner circle, passing through the annular region in the middle of the two hedges ($r_2 - r_1 = 1m$). To reduce the computational burden, a 2D section is taken as representative of the axially symmetric domains, Fig. 4. Under the quiescent irrota-

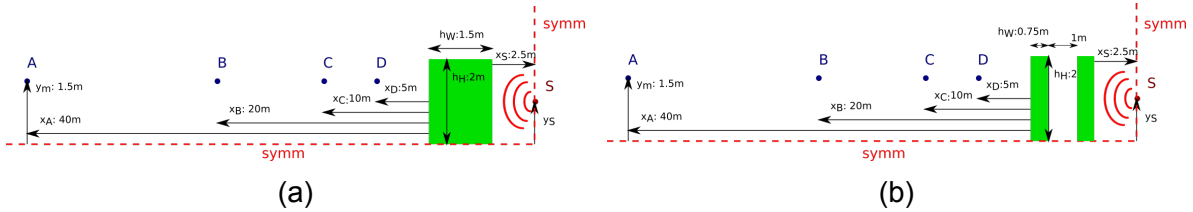


Figure 4: Single- and two-layer hedges, (a) and (b) respectively, numerical analysis sketch.

tional and homentropic fluid hypothesis, the small amplitude acoustic perturbations are held by the D'Alembert operator ($\square p = S$). The wave equation is then Fourier-transformed and solved in the frequency domain. A FEM-BEM combined approach is employed in order to set a multi-domain problem, in which the propagation properties of the hedge(s) domain, modeled with the FEM, are obtained from Eqs.(4) and (5), considering $\rho_0 = 1.21 \text{ kg/m}^3$ and $c_0 = 343 \text{ m/s}$. The use of the BEM for the exterior propagation automatically ensures the non-reflecting condition at infinity. An elementary point acoustic monopole of unitary amplitude is used to model the noise source ($S = \delta(\mathbf{x} - \mathbf{x}_S)$). The noise reduction effect of the green barrier is investigated for two vertical positions of the source $y_s = 1\text{m}$ and 2m , centered in the landing area, at a set of virtual receivers placed 40, 20, 10, and 5 m away from the outer edge of the hedges at 1.5 m from the ground, named A, B, C and D respectively. The application of the method of the images ensures the imposing of the symmetries of the problem. In this way, the ground is considered acoustically hard, as suggested in ISO 9613-2 for low porosity ground surfaces. Although this may be considered an oversimplification of its properties, considering the even remarkable effect by the ground is out of the scope of the present work. An additional set of simulations neglecting the presence of the ground is also performed.

For all the cases, the Insertion Loss is evaluated as

$$IL(\mathbf{x}) = 10 \log \frac{|p_F(\mathbf{x})|^2}{|p_H(\mathbf{x})|^2} \quad (12)$$

where p_F , also called the free field solution, is the result obtained from the free propagation of the monopole, only interacting with the ground when considered, and p_H is

the solution in the presence of the green barrier (and the ground). According to simulations, the single- and double-layer hedge barrier behave similarly, see Figs.5 and 6 for both source positions, suggesting that the overall barrier thickness is the driving parameter. A substantial shielding effect, growing with frequency, occurs mainly when the noise source is "inside" the barrier ($y_s = 1\text{m}$). Even if not shown in the presented figures, some tests have been performed comparing the JCAH with the classic JCA and the Delany-Bazley-Miki models; the three predict consistent attenuations, with almost identical trends and levels. The trend and the Insertion Loss values achieved in this situation positively compare to the experimental and numerical results shown in [13], where a reduction of around 8-10 dB at 1kHz and 18-30 dB at 10kHz is measured for two different hedges of thickness similar to the one here considered. An even better agreement is seen compared to the single-layer no-ground case, which might be more representative of the experiments cited, where the directivity of the employed acoustic source was intended to avoid the interaction with the soil. The level of match reached is encouraging in terms of validation of the method adopted in the present work for the extrapolation of the equivalent porous medium parameters for the hedges. The presence of the hard terrain introduces some oscillations in the IL graph, typically more severe for the receiver D, closer to the hedge, compatibly to the constructive and destructive interference paths created by the ground reflections. The main reductions in the shielding performance appearing in the IL spectrum are directly correlated to SPL dips in the free field solutions due to the mentioned destructive interference between direct and ground-reflected waves. These effects are intrinsically local in space and, moreover, the presence of a physical delay/attenuation by the ground (*i.e.*, a finite complex-valued ground impedance) in the reflected waves will have a dramatic impact on their importance. As expected, when the monopole source is at the same height as the upper edge of the hedge(s), the noise signal is subject to a less effective shielding effect by the barrier(s), especially for far receivers more also exposed to diffracted sound. However, the predicted attenuations are also remarkable for the less favorable source-receiver positioning, with an average IL of about 10dB.

5. Conclusions

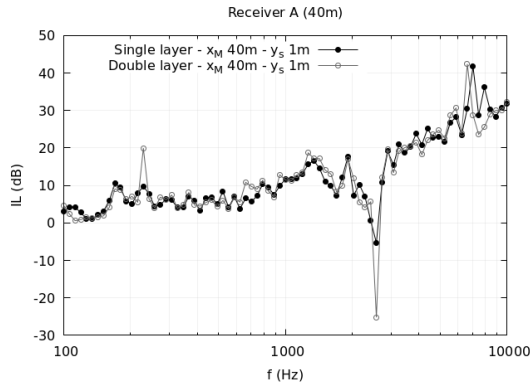
The use of natural elements such as hedges and brushes to reduce noise annoyance caused by commercial drone hubs in urban areas has been investigated through a proof-of-concept analysis. An image processing method has been developed to estimate the equivalent porous medium parameters for the evaluation of noise abatement capability of such greenery barriers, allowing the use of the JCAH model. The values obtained for the three driving parameters are in agreement with those present in the literature. The combination of the image processing and JCAH methods, when applied to plants, avoids the need for direct measuring of parameters otherwise hard to be quantified, such as tortuosity, flow resistivity, and the number of leaves. Numerical simulations predict significant noise reductions, growing with frequency up to 10kHz; attenuation around 10dB at 1kHz and up to 30dB from 6kHz and above are obtained. Comparing results from the single- and double-layer designs, it that the driving parameter for the attenuation is the overall thickness of the possibly seg-

mented barrier. Further validations also against experimental results and/or synthetic 3D models are envisaged in the next future for both the porous medium parameters estimation technique and noise reductions from hedges. Furthermore, simulations may be improved by involving more realistic geometries and ground properties, *i.e.* finite complex-valued impedances, at the cost of an increased computational burden.

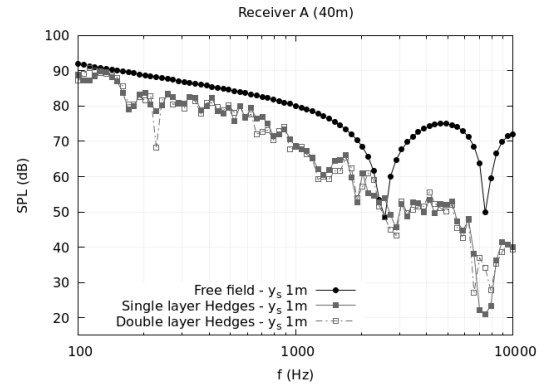
References

- [1] Straubinger, A, Rothfeld, R, Shamiyeh, M, Büchter, KD, Kaiser, J and Plötner, KO (2020) *An overview of current research and developments in urban air mobility—setting the scene for uam introduction*. Journal of Air Transport Management 87, 101852
- [2] Organization, ICA (2008) *Guidance on the balanced approach to aircraft noise management*. Technical report, ICAO
- [3] eVTOL news (2022). <https://evtol.news/aircraft>
- [4] Cohen, AP, Shaheen, SA and Farrar, EM (2021) *Urban air mobility: History, ecosystem, market potential, and challenges*. IEEE Transactions on Intelligent Transportation Systems 22(9), 6074–6087
- [5] Jung, S and Kim, H (2017) *Analysis of amazon prime air uav delivery service*. Journal of Knowledge Information Technology and Systems 12(2), 253–266. URL <http://dx.doi.org/10.34163/jkits.2017.12.2.005>
- [6] Rajendran, S and Srinivas, S (2020) *Air taxi service for urban mobility: A critical review of recent developments, future challenges, and opportunities*. Transportation research part E: logistics and transportation review 143, 102090
- [7] Hasan, S (2019) *Urban air mobility (uam) market study*. Technical report, Crown Consulting, Inc. Washington, DC, United States. URL <https://ntrs.nasa.gov/citations/20190026762>
- [8] Aylor, D (1972) *Noise reduction by vegetation and ground*. The Journal of the Acoustical Society of America 51(1B), 197–205. URL <https://doi.org/10.1121/1.1912830>
- [9] Van Renterghem, T, Botteldooren, D and Verheyen, K (2012) *Road traffic noise shielding by vegetation belts of limited depth*. Journal of Sound and Vibration 331(10), 2404–2425. ISSN 0022-460X. URL <https://www.sciencedirect.com/science/article/pii/S0022460X12000260>
- [10] Horoshenkov, KV, Khan, A and Benkreira, H (2013) *Acoustic properties of low growing plants*. The Journal of the Acoustical Society of America 133(5), 2554–2565. URL <https://doi.org/10.1121/1.4798671>
- [11] D'Alessandro, F, Asdrubali, F and Mencarelli, N (2015) *Experimental evaluation and modelling of the sound absorption properties of plants for indoor acoustic*

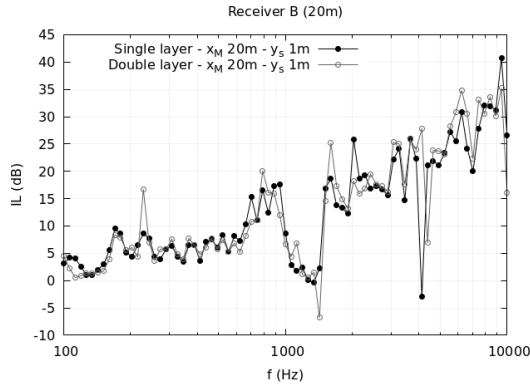
- applications*. Building and Environment 94, 913–923. ISSN 0360-1323. URL <https://www.sciencedirect.com/science/article/pii/S0360132315300196>
- [12] Miki, Y (1990) *Acoustical properties of porous materials-generalizations of empirical models-*. Journal of the Acoustical Society of Japan (E) 11(1), 25–28
- [13] Horoshenkov, K, Khan, A, Yang, H, Cheal, C, Smyrnova, J and Kang, J (2012) *In-situ characterization of hedges with a parametric acoustic transducer*. The Journal of the Acoustical Society of America 131(4), 3462–3462. URL <https://doi.org/10.1121/1.4709047>
- [14] *Wingcopter website*. <https://wingcopter.com/wingcopter-198#specs>. Accessed: 2022-04-29
- [15] *Swoop aero receives series a funding to deliver medical goods via drone*. <https://dronedj.com/2020/06/24/swoop-aero-receives-series-a-funding-to-deliver-medical-goods-via-drone/>. Accessed: 2022-04-29
- [16] *Swoop aero website*. <https://swoop.aero/kite>. Accessed: 2022-04-29
- [17] *Wing website*. <https://wing.com/how-it-works>. Accessed: 2022-04-29
- [18] Koiwanit, J (2018) *Analysis of environmental impacts of drone delivery on an on-line shopping system*. Advances in Climate Change Research 9(3), 201–207. ISSN 1674-9278. URL <https://www.sciencedirect.com/science/article/pii/S1674927818300261>
- [19] Horoshenkov, KV, Hurrell, A and Groby, JP (2019) *A three-parameter analytical model for the acoustical properties of porous media*. The Journal of the Acoustical Society of America 145(4), 2512–2517. URL <https://doi.org/10.1121/1.5098778>



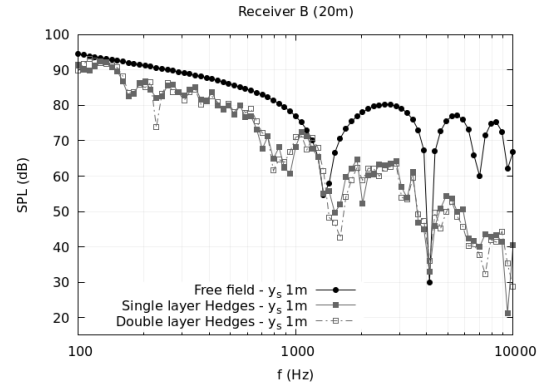
(a) IL at receiver A



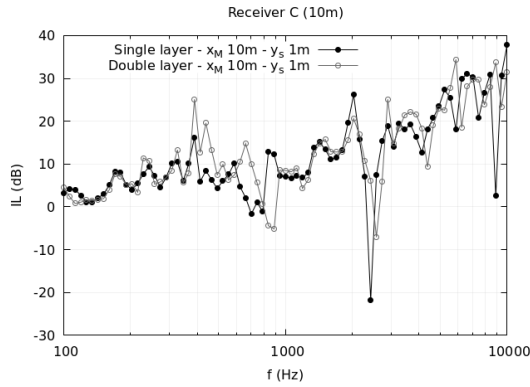
(b) SPL at receiver A



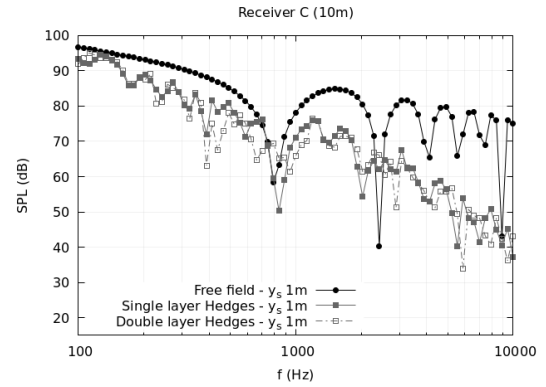
(c) IL at receiver B



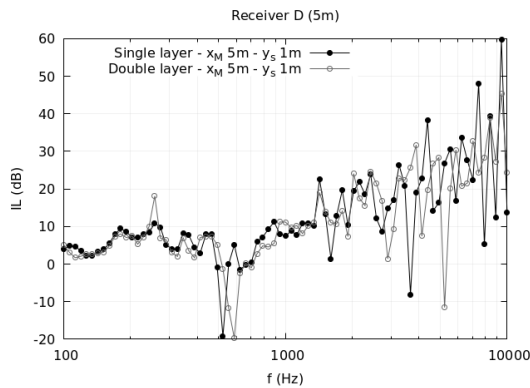
(d) SPL at receiver B



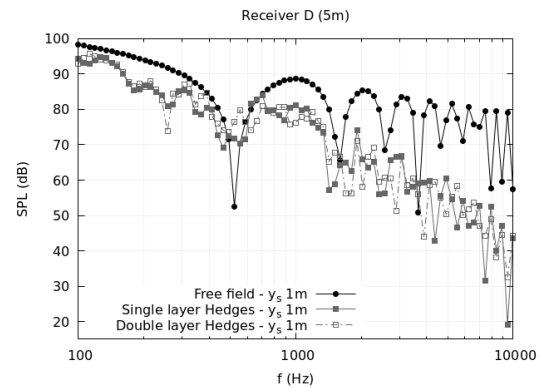
(e) IL at receiver C



(f) SPL at receiver C

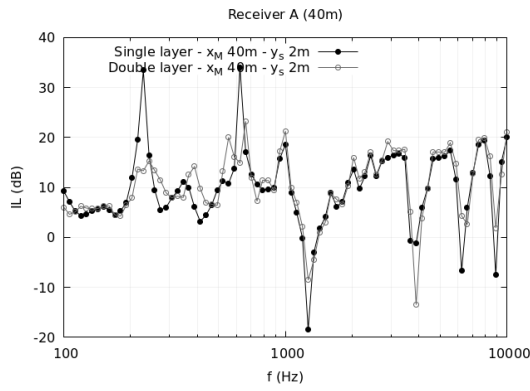


(g) IL at receiver D

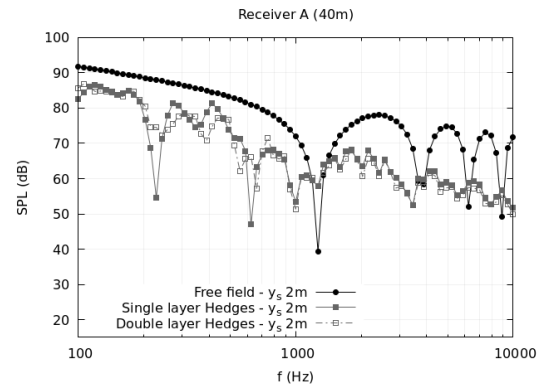


(h) SPL at receiver D

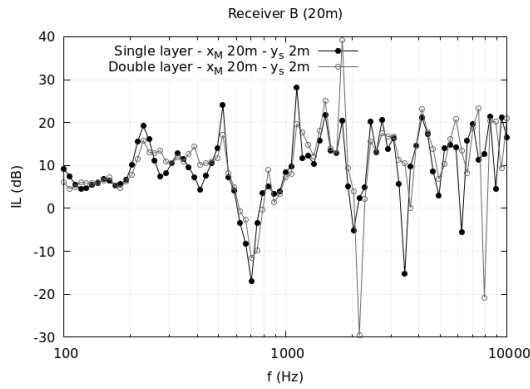
Figure 5: IL and SPL spectra at the virtual receivers, Single vs Double layer design, $y_s = 1m$.



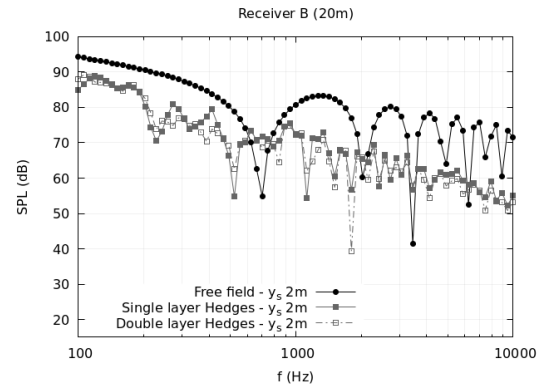
(a) IL at receiver A



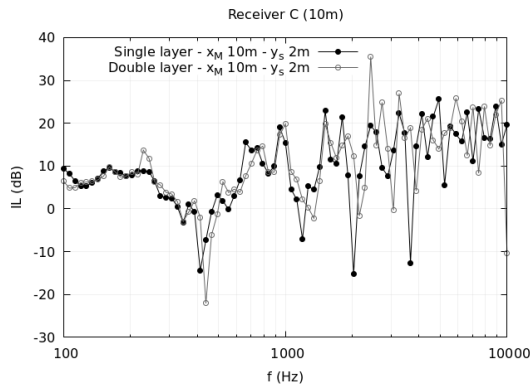
(b) SPL at receiver A



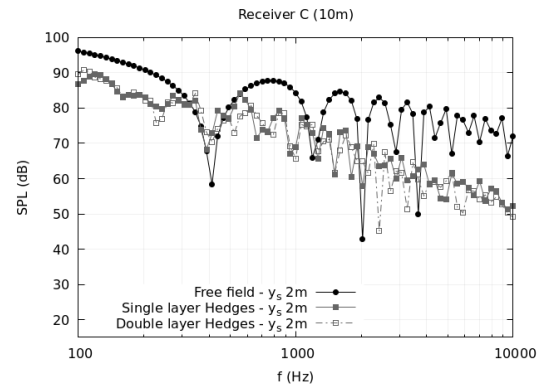
(c) IL at receiver B



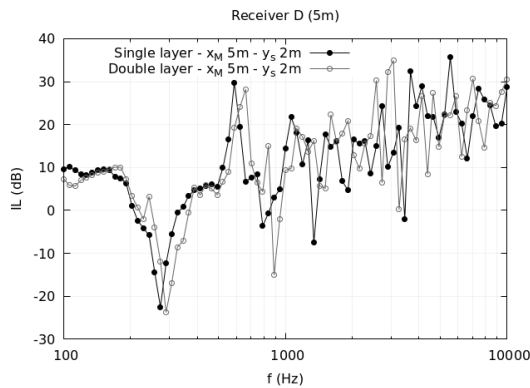
(d) SPL at receiver B



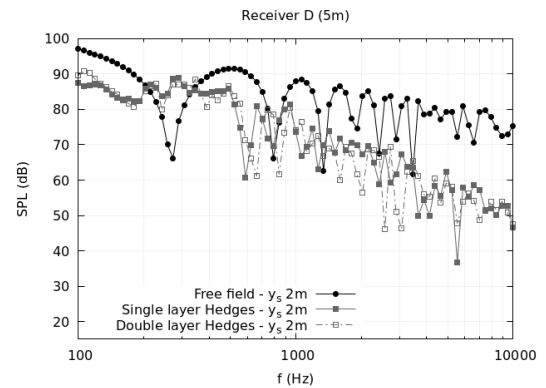
(e) IL at receiver C



(f) SPL at receiver C

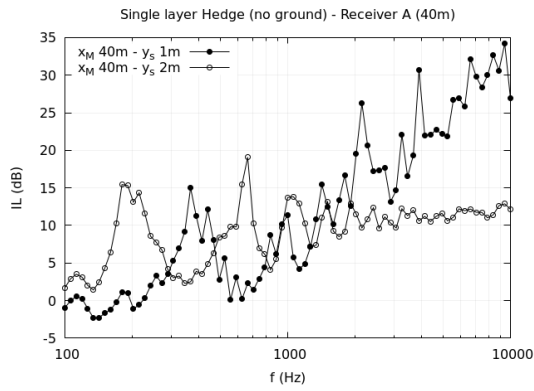


(g) IL at receiver D

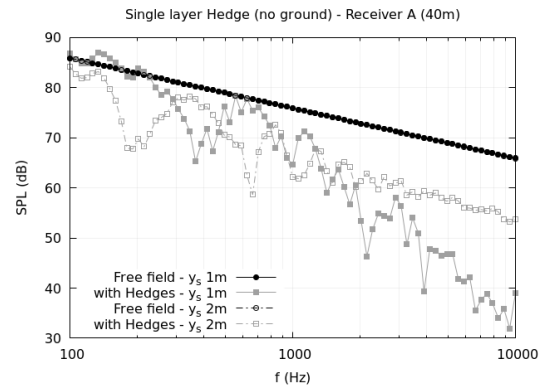


(h) SPL at receiver D

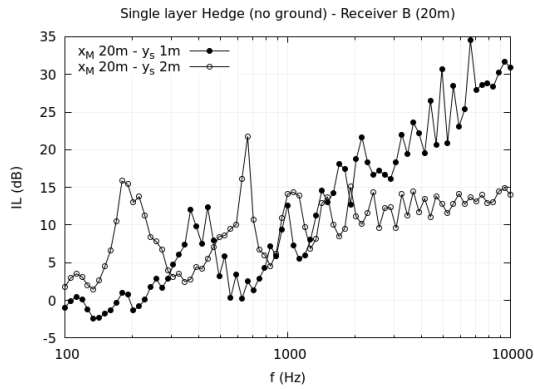
Figure 6: IL and SPL spectra at the virtual receivers, Single vs Double layer design, $y_s = 2m$.



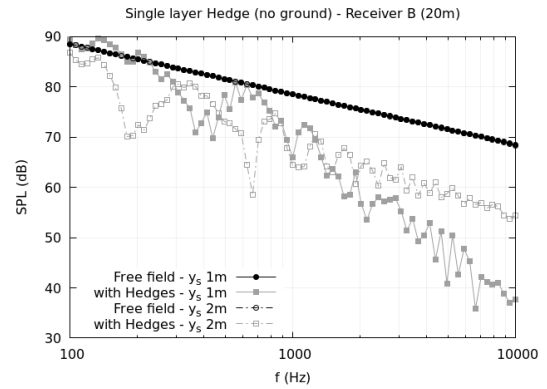
(a) IL at receiver A - no-ground



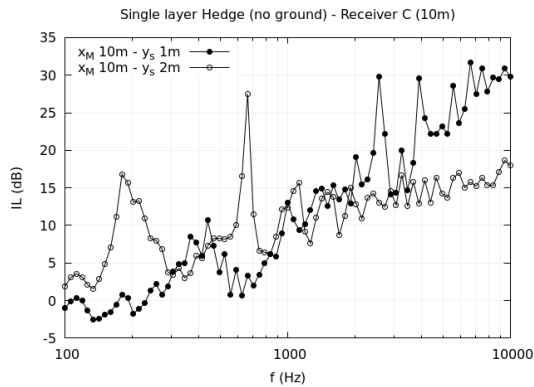
(b) SPL at receiver A - no-ground



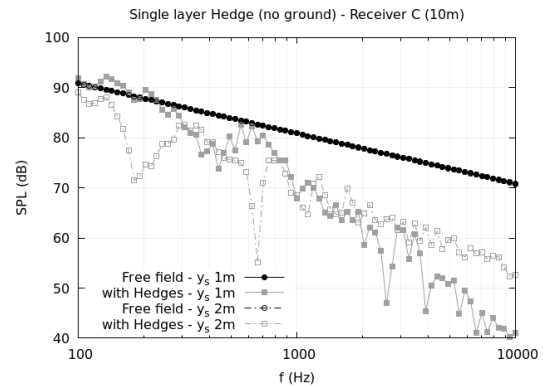
(c) IL at receiver B - no-ground



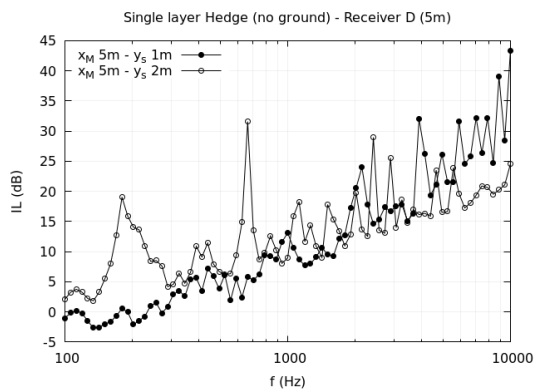
(d) SPL at receiver B - no-ground



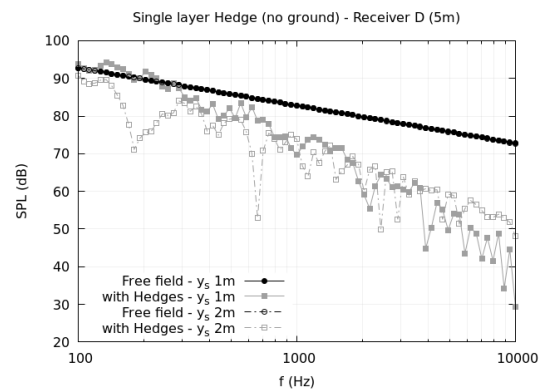
(e) IL at receiver C - no-ground



(f) SPL at receiver C - no-ground



(g) IL at receiver D - no-ground



(h) SPL at receiver D - no-ground

Figure 7: IL and SPL spectra at the virtual receivers, Single-layer hedge, no-ground simulations .